Pergamon

J. Aerosol Sci. Vol. 27, No. 3, pp. 359–382, 1996

0021-8502/96 $15.00 + 0.00

0021-8502(95)00533-1

THE WHITEHOUSE EFFECT—SHORTWAVE RADIATIVE FORCING OF CLIMATE BY ANTHROPOGENIC AEROSOLS: AN OVERVIEW

Stephen E. Schwartz

Environmental Chemistry Division, Brookhaven National Laboratory, Upton, NY 11973, U.S.A.

(*First received* 21 *February* 1995; *and in final form* 10 *July* 1995)

Abstract—Loadings of tropospheric aerosols have increased substantially over the past 150 yr as a consequence of industrial activities. These aerosols enhance reflection of solar radiation by the Earth–atmosphere system both directly, by scattering light in clear air and, indirectly, by increasing the reflectivity of clouds. The magnitude of the resultant decrease in absorption of solar radiation is estimated to be comparable on global average to the enhancement in infrared forcing at the tropopause due to increases in concentrations of CO_2 and other greenhouse gases over the same time period. Estimates of the aerosol shortwave forcing are quite uncertain, by more than a factor of two about the current best estimates. This article reviews the atmospheric chemistry and microphysical processes that govern the loading and light scattering properties of the aerosol particles responsible for the direct effect and delineates the basis for the present estimates of the magnitude and uncertainty in the resultant radiative forcing. The principal sources of uncertainty are in the loading of anthropogenic aerosols, which is highly variable spatially and temporally because of the relatively short residence time of these aerosols (ca. 1 week) and the episodic removal in precipitation, and in the dependence of light scattering on particle size, and in turn on relative humidity. Uncertainty in aerosol forcing is the greatest source of uncertainty in radiative forcing of climate over the industrial period. At the high end of the uncertainty range, the aerosol forcing is comparable to the anthropogenic greenhouse forcing, and substantially greater in industrialized regions. Even at the low end of the range, the aerosol forcing cannot be neglected in considerations of influences on climate over the industrial period. This uncertainty greatly limits the ability to draw empirical inferences of climate sensitivity to radiative forcing. Copyright © 1996 Elsevier Science Ltd

INTRODUCTION

The driving force of the Earth's climate is absorption of solar radiation at the surface and, to lesser extent, by the atmosphere. Absorption of solar radiation of course results in heating of the system. As the temperature of the system increases, it emits increasing amounts of thermal infrared radiation. To excellent approximation, the absorption of solar (shortwave) radiation by the Earth–atmosphere system is balanced by emission of thermal infrared (longwave) radiation, so that the earth may be considered to be in radiative equilibrium—more accurately, steady state—at least in global and annual average.

A schematic illustration of the Earth's radiation balance is given in Fig. 1. Here all the fluxes represent annual and global average values, in units of $W\,m^{-2}$. The average flux of shortwave solar radiation incident upon the Earth–atmosphere system is $1/4F_T \approx 343\,W\,m^{-2}$; F_T is the solar flux outside the atmosphere (the solar "constant"), about $1370\,W\,m^{-2}$. The factor of 4 results from the ratio of the area of the Earth to that of the subtended disk. Of this incoming solar radiation, a fraction $\bar{R} \approx 0.3$ is reflected, where $\bar{R}$ is the global-mean planetary albedo (Ramanathan, 1987; Ramanathan *et al.*, 1989); this flux corresponds to about $106\,W\,m^{-2}$. The principal contribution to the reflected shortwave radiation is from clouds; other contributions come from Rayleigh scattering by air, scattering by atmospheric aerosol particles, and surface reflectivity. The complement of the albedo $1 - \bar{R}$ corresponds to absorbed shortwave radiation and represents an average absorbed flux of $1/4F_T(1 - \bar{R}) \approx 237\,W\,m^{-2}$, that is matched, on an annual and global basis, by longwave emission.

Clouds, water vapor, and other infrared absorbing gases in the atmosphere, both absorb and emit longwave radiation. The presence of these substances in the atmosphere leads to

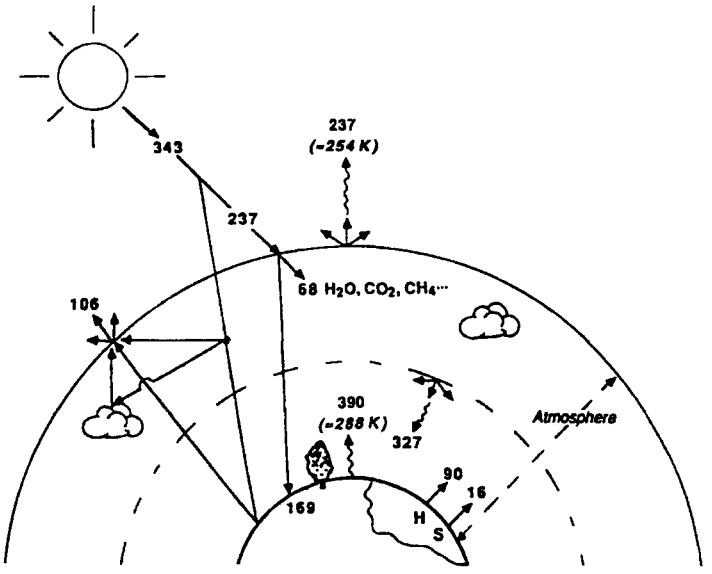

Fig. 1. Schematic (not to scale) of major fluxes constituting the radiation balance of the Earth–atmosphere system. Numbers represent global, annual average values in $W m^{-2}$. The shortwave flux incident at the top of the atmosphere, 343 $W m^{-2}$, represents one-fourth of the mean solar constant, taking into account the ratio of the area of the Earth relative to the area subtended by the planet. *H* and *S* denote latent and sensible heat fluxes from the Earth to the atmosphere, respectively. Modified from Ramanathan (1987).

radiation trapping between the Earth's surface and the atmosphere. Indeed, the flux of infrared radiation emitted at the surface of the Earth, ca. 390 $W m^{-2}$ global and annual average, substantially exceeds the outgoing infrared flux at the top of the atmosphere. Since these infrared-active constituents of the atmosphere are at high altitudes, they are cooler than the surface and therefore emit at a lower radiant intensity. Thus the mean emitted power of the Earth–atmosphere system, 237 $W m^{-2}$, corresponds to a lower black-body temperature (254 K) than does the emission flux at the surface, 390 $W m^{-2}$, which corresponds to a much more temperate value of 288 K. It must be stressed that the various fluxes indicated in the figure are averages of quantities that vary substantially, with location, season, and time of day.

The increase of surface temperature relative to the black-body temperature of the Earth–atmosphere system is known as the "greenhouse effect", by analogy to the supposed operating principle of greenhouses, i.e. transmission of shortwave radiation and blocking of longwave radiation, although in fact much of the effect of greenhouses is achieved by reduction of heat loss by convection and latent heat transport. This so-called greenhouse effect exerts a major influence on the Earth's climate, making the climate much more temperate than it would otherwise be. The moon, for example, is essentially at the same distance from the sun as is the Earth, but lacking an atmosphere containing infrared active gases (as well as surface water, with its large thermal mass), it has a much harsher climate that exhibits large temperature swings between day and night, with rapid radiative cooling at night.

As is now recognized, atmospheric concentrations of carbon dioxide and other infrared-active gases have increased substantially over the industrial period, with consequent resultant increases in their contribution to the longwave radiation balance at the surface. As is indicated in Fig. 2, the radiative influence of increased concentrations of long-lived infrared-active gases is calculated to be approximately 2.5 $W m^{-2}$, global and annual average. This secular change in radiative influence is denoted a "forcing" of the climate system; any resultant change in the climate system is denoted a response. Also indicated in the figure are the forcings due to increased concentrations of tropospheric ozone and

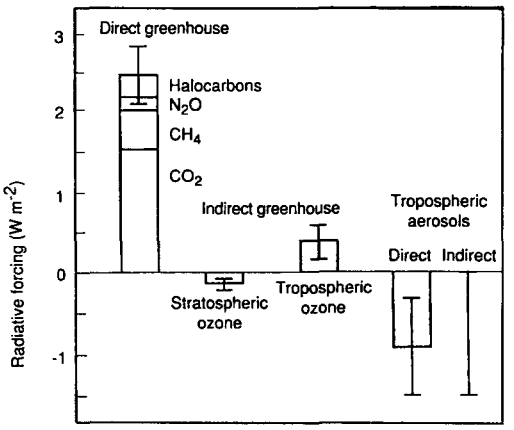

Fig. 2. Estimated magnitudes and uncertainties of anthropogenic contributions to radiative forcing of climate. From IPCC (1994).

decreased concentrations of stratospheric ozone. These forcings are considered indirect, in the sense that the perturbations in ozone concentrations result from atmospheric chemical reactions of other anthropogenic species (nitrogen oxides and hydrocarbons in the troposphere; chlorofluorocarbons in the stratosphere), and not directly, from emissions of ozone. It should be noted that the radiative influence of perturbations in water vapor and clouds is not indicated in the figure. Conventionally, the hydrological system is considered part of the climate system and, thus any changes in the loading and distribution of water in the atmosphere are viewed as part of the response of the climate system to the forcing arising from changes in atmospheric loading of the several greenhouse gases.

In view of the warming influence of greenhouse gases on the Earth climate system, it is generally assumed that increased concentrations of these gases will result in an increase in global mean temperature and possibly in other climatic changes. However, the magnitude of the response is not known either empirically or on the basis of models, in view of the complexity of the climate system, especially feedback effects involving water. This enhanced greenhouse effect is the subject of much concern in view of substantial effects on human society that might result from any change in climate. Consequently, much research is being directed to this phenomenon to allow it to be described more confidently in predictive models of the Earth climate. Principal components of this research are directed to improved description of (a) the perturbation in atmospheric loading of infrared-active gases that results from a given pattern of emissions, (b) the perturbation in forcing that results from a given increase in concentration, and (c) the climate response that results from a given perturbation in forcing. The present understanding of these phenomena is summarized in several reviews conducted under the auspices of the Intergovernmental Panel on Climate Change (IPCC, 1990, 1992, 1995).

A phenomenon which has received far less attention than the enhanced greenhouse effect, but which is now coming to be recognized as another major anthropogenic perturbation on radiative forcing of climate, is the enhancement of the shortwave albedo of the planet due to anthropogenic aerosols. As may be inferred from Fig. 1, an increase in planetary albedo will decrease the shortwave radiation absorbed by the Earth–atmosphere system and therefore exert a cooling influence on the planet. Aerosols affect the planetary albedo by scattering and absorbing shortwave radiation. In an early assessment of climate sensitivity to aerosol light scattering Coakley *et al.* (1983) examined the influence on surface temperature of a latitudinally dependent, hemispherically symmetric aerosol, for which they assumed a global mean optical depth (at 0.55 μm) of $0.125^{+0.05}_{-0.025}$

(Toon and Pollack, 1976) corresponding to a global mean change in radiative forcing of -0.7 to $-1.0\,W\,m^{-2}$; the negative sign indicates that the forcing exerts a cooling tendency. Calculation of temperature response with a general circulation model of the Earth atmosphere showed a latitudinally dependent influence, with a mean cooling of 2 to 3 K. At the time this aerosol and the resultant light scattering were thought to be predominantly of natural origin.

Subsequently it has become appreciated that loadings of aerosol particles in the troposphere have increased over the industrial period as a consequence of industrial emissions, similar to greenhouse gases. For example, measurements at Cape Grim Tasmania show that aerosol optical depth in "baseline" air in the Southern Hemisphere (SH), minimally perturbed by anthropogenic influences, is only about 0.05 (Forgan, 1987), well less than values that are characteristic of the more industrialized Northern Hemisphere (NH). Increased atmospheric loadings of particles can lead to an increase in the Earth's shortwave reflectivity. Two process have been identified, (1) the so-called "direct effect" of enhanced scattering of shortwave radiation due to increased concentrations of aerosol particles in clear (noncloud) air, and (2) the so-called "indirect effect" of enhanced cloud reflectivity resulting from increased multiple scattering in clouds containing higher concentrations of droplets owing to increased concentrations of aerosol particles that serve as nuclei for cloud droplet formation (cloud condensation nuclei, CCN).

By analogy to the term "greenhouse effect" the term "whitehouse effect" is introduced to refer to increased shortwave reflectivity arising from anthropogenic aerosols. The forcings due to anthropogenic aerosols are of opposite direction to that due to increased concentrations of greenhouse gases; i.e. they exert a cooling influence. The magnitude of these forcings are quite uncertain, but present estimates by the IPCC (1995) shown in Fig. 2 are such that at the high end of the uncertainty range the whitehouse forcing is comparable to the greenhouse forcing on global average. This would mean that the whitehouse forcing substantially exceeds the greenhouse forcing in regions proximate to industrial emissions. Even at the low end of the uncertainty range the whitehouse forcing is sufficiently great that it cannot be neglected in considerations of net anthropogenic influences on climate over the industrial period. The shortwave radiative influence of anthropogenic aerosols may thus be considered to be offsetting some, perhaps a great fraction, of the longwave radiative influence of anthropogenic greenhouse gases. However, this phenomenon has received much less attention by the climate research community than has the enhanced greenhouse effect, in part because of the more recent awareness of the phenomenon and in part because the phenomenon is more complex than the greenhouse effect and is not sufficiently well understood to be described with confidence.

Aerosol particles also absorb and emit longwave (infrared) radiation and, thus an enhanced concentration of aerosol particles might be thought to lead to a greenhouse influence that would offset some of the shortwave forcing of the aerosols. This effect is thought to be small, however, because the optical depth of aerosols decreases at longer wavelengths and because the aerosols are present mainly in the lower troposphere, where the atmospheric temperature, which governs emission, is close to that of the surface (Coakley *et al.*, 1983).

Aerosol species that are thought to contribute substantially to the whitehouse effect include sulfates, arising from emissions of SO_2 associated mainly with fossil fuel combustion, and organic aerosols arising from biomass combustion (Charlson *et al.*, 1991, 1992; Penner *et al.*, 1992, 1994; Jonas *et al.*, 1995). Nitrates and organics associated with industrial emissions may also be important, but the climate forcing by these species has received relatively little attention. These aerosol species have received much attention from the air pollution research community because of their possible contribution to acid deposition, health impairment, and visibility reduction; and the ability to describe the climate forcing relies heavily on the understanding gained from that research. In fact the direct effect is due to much the same physics that is responsible for the reduction of visibility due to anthropogenic aerosols, i.e. scattering of shortwave radiation. The difference is mainly one of geometry—the whitehouse effect results only from radiation which is scattered in the

upward direction and which thereby leaves the Earth–atmosphere system. The light scattering that gives rise to the whitehouse effect is often readily visible from high flying commercial aircraft as an apparent brightening or whitening of the surface due to diffuse scattering of solar radiation in the lower troposphere. Occasionally this upward scattered radiation can be so bright as to make it difficult to see or discern features of the surface, even in the absence of any clouds.

The subject of aerosol radiative influences on climate is of great current interest. Attention is called to several recent publications. The Proceedings of the 1994 Dahlem Workshop on Aerosol Forcing of Climate (Charlson and Heintzenberg, 1995) contains 15 chapters dealing with all aspects of this phenomenon as well as group reports summarizing the present knowledge and knowledge gaps. The 1995 IPCC report on Radiative Forcing of Climate Change contains a full chapter dealing with aerosol radiative forcing (Jonas *et al.*, 1995). Attention is called also to a review of the dynamics of tropospheric aerosols by Pandis *et al.* (1995) and to a review by Andreae (1995) that summarizes aerosol forcing especially by substances other than sulfate, and with examination of historical trends. For a recent review of the indirect forcing see Schwartz and Slingo (1995). The radiative influence of incremental cloud droplets has recently been examined also by Platnick and Twomey (1994).

The purpose of the present article is to describe the processes responsible for the direct forcing and to examine estimates of the magnitude of this forcing, with emphasis on identifying the reasons for the great uncertainties in these estimates. In order for the magnitude of the whitehouse effect to be accurately evaluated, the processes that control this magnitude must be well characterized. Much of the uncertainty rests in aspects of aerosol science that govern the loading and light scattering properties of tropospheric aerosols.

ESTIMATING THE FORCING

An initial approach to estimating the magnitude of the direct forcing due to anthropogenic aerosols is given by a box-model description of the phenomenon (Charlson *et al.*, 1992; Penner *et al.*, 1994). Although such a model is incapable of describing the geographical distribution of the forcing and of accounting for correlations among controlling variables, it is a useful first approximation, especially as the forcing is linear in aerosol loading for an optically thin aerosol in which single scattering dominates, and is thus independent of the details of the atmospheric distribution of the material.

To illustrate this approach we evaluate the shortwave forcing by anthropogenic sulfate aerosol. This model yields for the area-average shortwave forcing $\overline{\Delta F_R}$ resulting from an increase in sulfate aerosol concentration:

$$\overline{\Delta F_R} = -\tfrac{1}{2} F_T (1 - A_c) T^2 (1 - R_s)^2 \bar{\beta} \alpha_{SO_4^{2-}}^{RH_r} f(RH) \overline{B_{SO_4^{2-}}} . \quad (1)$$

The negative sign denotes that the forcing represents a cooling tendency; the factor of $\frac{1}{2}$ is due to only half the planet being illuminated at a given time. The symbols in the equation are defined as follows:

F_T is the solar constant, i.e. mean solar radiative flux at distance of the Earth to the sun;

A_c is the fractional cloud cover in the area of concern; the factor $(1 - A_c)$ is introduced because the albedo enhancement is applicable only for cloud-free regions;

T is the fraction of incident or scattered light transmitted through the atmosphere above the aerosol layer;

R_s is the albedo of the underlying surface; the factor $(1 - R_s)^2$ takes into account multiple reflection between the surface and the aerosol layer;

$\bar{\beta}$ is the fraction of the radiation scattered upward by the aerosol, averaged over the sunward hemisphere;

$\alpha_{SO_4^{2-}}^{RH_r}$ is the light-scattering mass efficiency of sulfate aerosol, i.e. scattering coefficient per sulfate mass, at a reference low relative humidity ($RH_r = 30\%$);

$f(RH)$ is the relative increase in scattering cross-section at ambient RH;

$\overline{B_{SO_4^{2-}}}$ is the mean column burden of sulfate resulting from anthropogenic emissions.

Table 1. Evaluation of global mean direct radiative forcing due to anthropogenic sulfate aerosol*

Quantity	Value	Units	Uncertainty factor
F_T	1370	$W\,m^{-2}$	—
$1 - A_c$	0.4	—	1.1
T	0.76	—	1.15
$1 - R_s$	0.85	—	1.1
$\bar{\beta}$	0.29	—	1.3
$\alpha_{SO_4^{2-}}^{RH_r}$	5	$m^2\,(g\,SO_4^{2-})^{-1}$	1.5
$f(RH)$	1.7	—	1.2
Q_{SO_2}	80	$Tg\,S\,yr^{-1}$	1.15
$Y_{SO_4^{2-}}$	0.40	—	1.5
$\tau_{SO_4^{2-}}$	0.020	yr	1.5
A	5×10^{14}	m^2	—
$\overline{\Delta F_R}$	-1.1	$W\,m^{-2}$	2.4

*After Charlson *et al.* (1992) and Penner *et al.* (1994).

Equation (1) displays the treatment of the radiative forcing. The column burden of sulfate in principle might be obtained by direct measurement, but in view of the variability of this quantity, as discussed below, can be obtained only by modeling the atmospheric chemistry. Again, restricting consideration to a box model, one obtains for the mean column burden:

$$B_{SO_4^{2-}} = Q_{SO_2} Y_{SO_4^{2-}} \tau_{SO_4^{2-}} / A, \tag{2}$$

where

Q_{SO_2} is the source strength of anthropogenic SO_2;

$Y_{SO_4^{2-}}^{RH_r}$ is the fractional yield of emitted SO_2 that reacts to produce sulfate aerosol; since equation (1) is based on the mass of sulfate ion, a further factor of 3 must be included to account for the ratio of the molecular weight of sulfate to that of sulfur (96/32 = 3),

$\tau_{SO_4^{2-}}$ is the mean residence time of sulfate aerosol in the atmosphere;

A is the area of the geographical region to which the calculation is applied, e.g. the entire Earth or the Northern Hemisphere.

Equations (1) and (2) may be combined to give

$$\overline{\Delta F_R} = -\tfrac{1}{2} F_T (1 - A_c) T^2 (1 - R_s)^2 \bar{\beta}\, \alpha_{SO_4^{2-}}^{RH_r} f(RH) Q_{SO_2} Y_{SO_4^{2-}} \tau_{SO_4^{2-}} / A. \tag{3}$$

Equation (3) has the advantage of explicitly delineating the dependence of $\overline{\Delta F_R}$ on all of the variables on which it depends, thereby allowing identification of key uncertainties. Estimates of values of the several parameters in equation (3) are given in Table 1, which is based on Charlson *et al.* (1992). The magnitude of global mean direct radiative forcing due to sulfate aerosol evaluated by this equation with the parameters given in Table 1, is about $-1\ W\,m^{-2}$. Similar global average results are obtained in calculations based on geographical distributions of these aerosols calculated with chemical transport models which explicitly show the geographical distribution of this forcing, concentrated in the vicinity of industrial regions of the Northern Hemisphere (Charlson *et al.*, 1991; Kiehl and Briegleb, 1993).

Also given in Table 1 are somewhat subjective estimates of the uncertainties associated with the several factors in equation (3). The overall multiplicative uncertainty given in Table 1 is evaluated as $f_t = \exp[\sum(\log f_i)^2]^{1/2}$, where the f_i are the multiplicative uncertainties estimated for the individual factors in equation (3). Key sources of uncertainty are microphysical factors (scattering efficiency and upscatter fraction and the dependence of these quantities on particle size and relative humidity, RH) and atmospheric chemistry factors (yield and residence time). Propagation of the several uncertainties under assumption that they are uncorrelated leads to an estimated uncertainty in the forcing of a factor of about 2.4; i.e. a factor of almost 6 between extremes. The possibility has been noted,

however, of correlation of the pertinent aerosol properties, i.e. mass scattering efficiency, upscatter fraction, and RH dependence, that would lead to a reduction in the overall uncertainty (Boucher and Anderson, 1995).

A similar treatment has been given for direct radiative forcing by aerosols resulting from biomass combustion (Penner *et al.*, 1992, 1994), with the resulting estimate about $-0.6\ \mathrm{W\,m^{-2}}$ and with similar factor-of-two uncertainty. A further source of uncertainty associated with biomass combustion aerosol forcing is the history of emission trends, which do not necessarily follow those of anthropogenic sulfates. No systematic estimates have been given of shortwave forcing by nitrate aerosols, another major class of light scattering anthropogenic aerosols. Although nitrates are a major contributor to aerosol loading and light scattering in regions proximate to sources (e.g. Sloane, 1983; White, 1991; Veefkind *et al.*, 1996) it may be speculated that these materials contribute less to radiative forcing on a global scale because of the volatility of nitrate (as HNO_3) that returns the material to the gas phase once the aerosol has been diluted by atmospheric dispersion processes. However, this has yet to be examined systematically. Similar uncertainties govern estimates of the climate forcing due to aerosols from biomass combustion and other sources. It is clear that such great uncertainty dominates the uncertainty of anthropogenic climate forcing over the industrial period indicated in Fig. 2.

In view of the relatively developed state of knowledge regarding sulfate aerosols, the following discussion focuses on radiative forcing by this class of aerosols. However, it should be kept in mind that this is only a subset of anthropogenic aerosols, and that other substances undoubtedly contribute both to the forcing and to the overall uncertainty of radiative forcing over the industrial period. This discussion is conveniently organized according to the atmospheric chemistry processes that control aerosol loading, equation (2), and radiative processes that control the forcing for a given aerosol loading, equation (1).

PROCESSES AND PROPERTIES GOVERNING THE FORCING

Atmospheric chemistry

In principle if the mean loading or column burden of anthropogenic sulfate were known empirically, as is the case for the anthropogenic enhancement in greenhouse gas concentrations, the known values could be used in place of the quantities calculated as indicated in equation (3). However, in contrast to situation for the greenhouse gases, sulfate aerosol is quite nonuniformly distributed in space and time, as a consequence of the relatively short atmospheric residence time of this species. An example of the temporal variability in sulfate concentration is shown in Fig. 3, which shows concentrations of sulfate aerosol measured over a one year period at Whiteface Mountain, some 400 km north of New York City and 1.5 km above sea level. Here the measurements represent 24-hour average concentrations; measurements on successive days are connected by vertical lines. It is seen that there is great day-to-day variability in the concentrations. The coefficient of variation in the data (standard deviation/average) is 135%. Even on sucessive days the variation in 24-hour concentrations can be substantial, occasionally by as much as an order of magnitude. The variability is dominated by synoptic-scale meteorological variability—precipitation and wind direction and speed—together with episodicity in removal, which is dominated by removal in precipitation. It is clear that variability such as this virtually precludes determining the atmospheric loading simply by measuring concentrations.

In principle, an attractive approach to mapping out the distribution of aerosol loading would be by means of satellite-borne instruments. However, to date only a few satellites have carried instruments specifically designed for aerosol measurements, and those are directed mainly to examination of stratospheric aerosol (SAGE, stratospheric aerosol and gas experiment; SAM, stratospheric aerosol measurement; McCormick *et al.*, 1979). In the absence of instruments designed for aerosol measurements, reliance has been made on alternative approaches, mainly the AVHRR (advanced very high resolution radiometer) on the NOAA polar orbiting satellites (Rao *et al.*, 1988). However, this approach is limited to

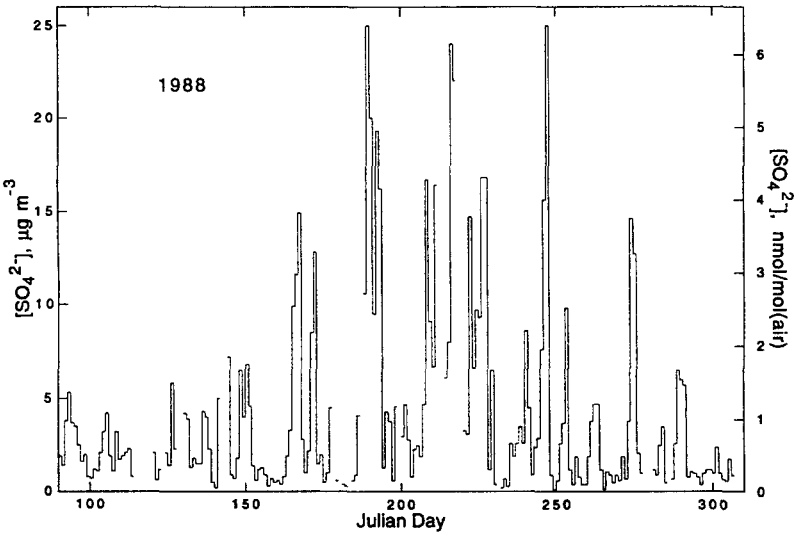

Fig. 3. Time series of 24-hour average concentrations of aerosol sulfate at Whiteface Mountain, NY, 1500 m altitude. Concentrations are expressed as μg sulfate per standard cubic meter (reference temperature 293 K; reference pressure 1 atm). Measurements on successive days are connected by lines. Data provided by L. Husain, New York State Department of Health; see Husain and Dutkiewicz (1990).

measurements over oceans, because of the high and variable surface radiance over land scenes, and even over oceans retrieval of path radiance and conversion to aerosol optical depth is subject to large uncertainty (Wagener *et al.*, 1996). Prospective instruments that can improve the ability to map out aerosol distributions have been briefly described by Penner *et al.* (1994) and Hansen *et al.* (1990) and in more detail by Hansen *et al.* (1993).

Given that such an approach is not yet available, one must resort to models of the atmospheric chemistry governing sulfate aerosol to infer the atmospheric loading of this material. Such models must represent the key processes that constitute the atmospheric "life cycle" of this material, i.e. formation and removal processes, either by means of box models that simulate these processes or by models of higher dimension that represent transport as well. Despite the importance of the atmospheric chemistry of sulfates relative to acid deposition and other air pollution issues and despite considerable research in this area, estimates of the several parameters needed to describe atmospheric loadings remain rather uncertain, as indicated by the uncertainties given in Table 1. Here the important sources of uncertainty in atmospheric loading of sulfate are briefly reviewed.

Most sulfate in the atmosphere is formed by atmospheric oxidation of emitted SO_2 and, thus the key quantities required to describe the source strength of sulfate are the emission strength of anthropogenic SO_2 (Q_{SO_2}) and the fraction of emitted SO_2 that is converted to sulfate aerosol (yield, $Y_{SO_4^{2-}}$). The uncertainty in global emissions of SO_2 indicated in Table 1 is fairly small; for recent survey of emissions see Spiro *et al.* (1992). The fractional conversion of SO_2 to sulfate versus removal as SO_2 (mainly by dry deposition) is much more uncertain. Atmospheric oxidation of SO_2 occurs by gas-phase reaction (with OH radical) and by aqueous-phase reaction in clouds (mainly with H_2O_2 and O_3). A major unresolved question is the extent of in-cloud reaction. The in-cloud reaction of SO_2 with H_2O_2 is rapid and is thought to proceed essentially to completion, as limited by the amount of the reagent in lower concentration (Daum *et al.*, 1984; Daum, 1988; Mohnen and Kadlecek, 1989; Burkhard *et al.*, 1994). Thus to first approximation the extent of reaction is limited by the amount of SO_2 that is processed by clouds, but not exceeding the amount of H_2O_2 present. A related issue is the amount of sulfate that is returned to the atmosphere as aerosol versus that removed by precipitation in the same event as that in which it was produced.

Removal of sulfate from the atmosphere is characterized by a mean residence time ($\tau_{SO_4^{2-}}$). Removal occurs primarily by nucleation scavenging of aerosol particles during cloud formation, followed by deposition of the dissolved material in precipitation; the (1/*e*) time for removal of accumulation-mode particles by dry deposition is several tens of days (e.g. Slinn, 1983). Light-scattering aerosol generally, and sulfate in particular, appears to be taken up into cloudwater with high efficiency (ten Brink *et al.*, 1987) and, thus it appears that the fate of sulfate aerosol depends on the frequency of uptake into precipitating clouds, with the fate of the sulfate being the same as the cloudwater in which it is dissolved. Unfortunately the rate of this process is not well established. Inferences of $\tau_{SO_4^{2-}}$ based on concentrations of sulfate in air or precipitation are necessarily ambiguous because of continuous and distributed sources and because of sulfate formation by atmospheric oxidation of SO_2 (Schwartz, 1989). From the decrease in sulfate concentration in precipitation with distance over the North Atlantic, Whelpdale *et al.* (1988) inferred a (1/*e*) decay distance of 2400 km. For a mean transport velocity of 300 to 500 km per day (Summers and Young, 1987), the corresponding mean residence time is 5 to 8 days.

An independent estimate of the mean residence time of accumulation mode tropospheric aerosols can be gained from a study of the decay of atmospheric ^{137}Cs in the weeks following the accident at the Chernobyl nuclear generating station in Ukraine, in 1986. The atmospheric loading of this radionuclide during this period derived almost entirely from that accident. The emitted ions rapidly attached to accumulation mode aerosol particles; the activity median radius of ^{137}Cs during this period was 0.2 to 0.3 μm (Bondietti *et al.*, 1988); cf. average mass-median aerodynamic radius of continental sulfate of 0.26 μm reported in an extensive review of sulfate size distributions (Milford and Davidson, 1987). Consequently the decay of this material in the atmosphere may be considered a surrogate for rate of removal of accumulation mode aerosol by atmospheric deposition processes. Concentrations measured at several midlatitude stations in Europe and Asia were reported by Cambray *et al.* (1987). The data from the several sites could be plotted on a single semi-logarithmic plot, with mean residence time of about 6 to 8 days, Fig. 4. To the extent that the removal processes governing these aerosols can be taken as representative of those of anthropogenic sulfate, then the mean residence time inferred from these studies can be ascribed to that sulfate. Actually, such a value may be somewhat high for the mean residence time of sulfate aerosol, because during the several week period, the ^{137}Cs remaining in the atmosphere was undoubtedly at somewhat greater mean altitude than would be representative of sulfate aerosol in the atmosphere. The greater altitude would be expected to lead to a decrease in removal rate and thus an increased mean residence time (Benkovitz *et al.*, 1994). Nonetheless, the mean residence time derived from this analysis is certainly consistent with other estimates noted above.

The atmospheric loading of sulfate has been calculated in a number of regional- to global-scale models of varying degrees of sophistication, as summarized in Table 2. These models can be used to infer the pertinent atmospheric chemistry variables in equation (2). Alternatively the output of these models can be used as input to evaluations of radiative forcing (Charlson *et al.*, 1991; Kiehl and Briegleb, 1993; Taylor and Penner, 1994; Mitchell *et al.*, 1995; Boucher and Anderson, 1995; Cox *et al.*, 1995). Either way it is necessary to evaluate the accuracy of the modeled concentrations by comparison with observations. Such evaluations, albeit necessarily restricted to limited space and time domains, lend confidence to the use of the modeled concentration fields for evaluation of radiative forcing and provide a sense of the uncertainty in the estimated loadings. The performance of the atmospheric sulfur cycle model of Langner and Rodhe (1991), which was driven by monthly average meteorology, may be considered typical of the state of the art. Maximum annual average modeled sulfate mixing ratios in Europe and North America were 3 and 2 ppb, respectively, compared to observed values of 3.5 and 2.5 ppb, respectively. In remote locations the agreement between model and observations was "better than a factor of two for most cases". However, comparison of monthly results (Langner *et al.*, 1993) indicated the month-to-month variability in the model to be much weaker than is observed and to exhibit differences in seasonal patterns.

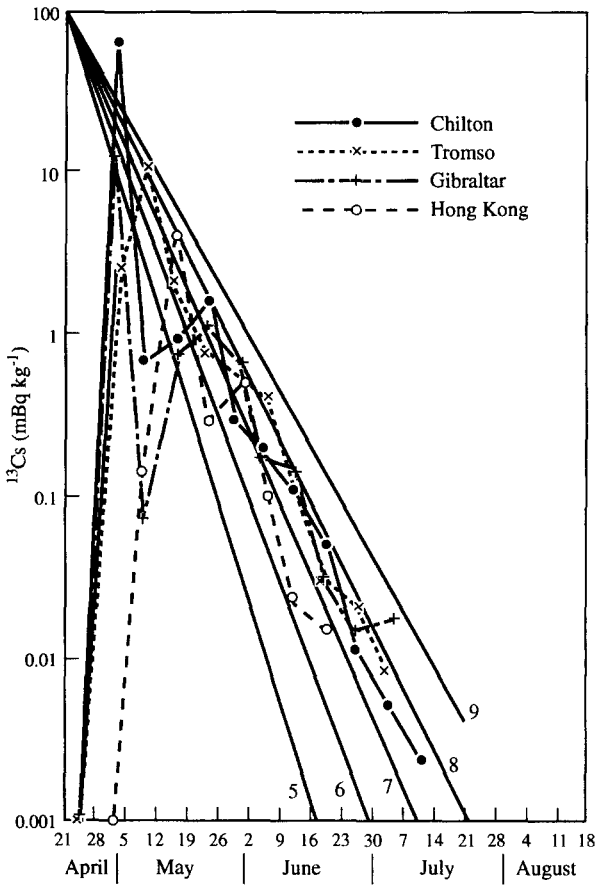

Fig. 4. Semi-logarithmic plot of weekly concentrations of ^{137}Cs at several midlatitude Northern Hemisphere locations in the several weeks following the accident at the Chernobyl (Ukraine) nuclear power station. Straight lines indicate concentration profiles for mean atmospheric residence times of 5 to 9 days. Modified from Cambray *et al.* (1987).

A somewhat different approach was taken by Benkovitz *et al.* (1994), who suggest that the high spatial and temporal variability of sulfate loadings means that a much more sensitive test of model performance will be gained by driving the model with observation-derived meteorology and conducting short-term comparisons of modeled and observed concentrations. For a one-month model study encompassing North America, the North Atlantic, and the European continent some 1700 daily concentrations were compared. The model was within a factor of 2 of the observations in 44% of the cases and within a factor of 3 in 66% of the cases. The average modeled/observed concentration ratio was 1.2, 0.85, 0.58, and 0.37 for observed concentrations < 0.5, 0.5–1, 1–5, and 5–10 ppb, respectively. The model also fairly accurately represented day-to-day variability of measured concentrations at 43 stations where time series comparisons could be made. The investigators noted that the departures between model and observations should not necessarily be attributed entirely to the model, as the observations are point measurements, whereas the model concentration is meant to represent a much larger area, in this case roughly 100×100 km. The mean sulfate yield inferred from the model was 53% and the mean residence time 4.7 days (0.013 yr), comparable to the values given in Table 1.

It may be noted that short-term comparisons, while lending confidence to the model, may constitute an overly stringent test of model skill for the purpose of radiative forcing estimates, since errors in transport winds may misrepresent the concentration at any given location, even if the atmospheric chemistry and resultant loading is accurately represented on the average.

Table 2. Regional to global scale models for aerosol sulfate

Reference	Scale; horiz. grid	Vert. levels	Met driver	Emissions	Gas-phase chemistry	Aqueous chemistry	Dry Dep., $cm\,s^{-1}$ SO_2 SO_4^{2-}	Wet removal
Rodhe and Isaksen (1980)	Global; 2-D; 10°	~ 20	Clim avg.	Ant SO_2 DMS	Chemical mechanism	Max 0.25 d^{-1}	0.6 0.2	Max 0.3 d^{-1}
Venkatram and Karamchandani (1986)	100 km	7	Weather forecast model	SO_2, SO_4^{2-} NO_x, HC	Chem. mech. 50 species	Chem. mech. 13 species	Calculated from meteorology	"Bulk water" technique
Giorgi and Chameides (1986)*	Global; 7.5° × 4.5°	9	GCM output	Constant	No	No	No	Local removal efficiency
Chang *et al.* (1987)	2400 × 2400 km; 80 km	6	Mesoscale met model	SO_2, SO_4^{2-} NO_x, HC	Chem. mech. 36 species	Kinetic chem. mech.	Calculated from meterology	Grid avg. precip. rate × avg. cloud water conc.
Iverson *et al.* (1989), Sandnes (1993)	6000 × 5500 km; Lagrange	1	Weather forecast model	SO_2, SO_4^{2-} NO_x, NH_3	Explicit S and N; paramet. oxidant reactions	Combined with gas-phase chemistry	SO_2 calc. from meteorology; SO_4^{2-}: 0.1	Scavenging ratios
Hass *et al.* (1991)	Modified version of Chang *et al.* (1987) (different transport-solving algorithm)							
Carmichael *et al.* (1991)	1600 × 7000 km; 80 km	11	Objective analysis of observations	SO_2, SO_4^{2-} NO_x, HC	Chem. mech. 55 species	Chem mech. 31 reactions	Calculated from meteorology	Nucleation + first-order scavenging
Langener and Rodhe (1991)	Global; 10°	10	Mon avg. and statistical	Ant SO_2 DMS	Fixed rate constants for SO_2 and DMS	Timescale paramet.	Met. modified Base: 0.8, 0.6, 0.1 0.2	Efficiency parameterization
Erickson *et al.* (1991)	Global; Lagrange	NA	GCM output	Ant SO_2 DMS	SO_2: 3-D conv. time; DMS: immediate	No	None 0.05	Rain × removal efficiency (1 and 0.3 cm^{-1})
Luecken *et al.* (1991)	20 000 × 7000 km; 5° × 3°	14	GCM	Ant SO_2 DMS	SO_2: avg. rate const; DMS: immediate	H_2O_2: reactant limited; O_3: avg. rate const.	0.8 0.4	Fractional removal cloud water to total precipitation
Tarrason and Iversen (1992)	Global; 300 km	10	12-h NMC analyses	Ant SO_2 Prim SO_4^{2-}	Linear rate by lat. and season	Combined with scavenging	Met. modified Base: 0.8 0.1	Rain × removal efficiency
Balkanski *et al.* (1993)*	Global; 4° × 5°	9	GCM output	^{222}Rn	No	No	Micromet. and met. data	Scavenging eff. (50, or 100%)
Taylor and Penner (1994)	Global; 7.5° × 4.5°	12	12-h avg. of GCM output	Ant SO_2	SO_2 + OH; [OH] from 2-D model	Conv. rate seasonal $f([OH]^2)$	0.8	Rain × scavenging coeff. (0.8)
Benkovitz *et al.* (1994)	20 000 × 7000 km; 1.125°	15	ECMWF 6 h forecast	Ant SO_2 Prim SO_4^{2-} DMS, H_2S	SO_2 + OH; DMS + OH; [OH] from 3-D model	H_2O_2: reactant limited; O_3: avg. rate const.	Calculated from meteorology	Fractional removal cloud water to total precipitation

*Not a model for aerosol sulfate; included because of treatment of transport and deposition of accumulation mode aerosol.

It is of interest to evaluate the atmospheric loading of sulfate with the parameters given in Table 1. This evaluation yields for the global average column burden of anthropogenic sulfate 3.8 mg m^{-2}. For a scale height of 2 km, this burden translates to a concentration of 1.9 μg m^{-3} or mixing ratio of 0.49 nmol mol$_{air}^{-1}$. For 90% of anthropogenic emissions in the Northern Hemisphere (NH), these quantities for the NH are 6.9 mg m^{-2}, 3.5 μg m^{-3}, and 0.88 nmol mol$_{air}^{-1}$, respectively. The latter quantities are comparable, within the rather broad uncertainty estimates of the model, with measurements summarized by Schwartz (1988) and Langner *et al.* (1993).

In summary, description of the loading of atmospheric sulfate, including its time and space dependence is a major source of uncertainty in estimating the radiative forcing due to anthropogenic sources of this material, with an uncertainty that must be viewed as a factor of two or more. Obviously any uncertainty in this quantity transfers directly into uncertainty in the shortwave forcing by this aerosol species.

Aerosol radiative properties

A second contribution to the uncertainty in direct forcing by sulfate aerosols is associated with the quantities relating forcing to atmospheric loading of this material, as indicated in equation (1). These quantities include the scattering efficiency of the material, $\alpha_{SO_4^{2-}}^{RH_r}$, the relative humidity dependence of this scattering efficiency f(RH), and the fraction of the scattered radiation is scattered into the upward hemisphere β. Here these quantities are briefly described and their dependence on aerosol microphysical properties outlined. The influence of particle size, composition, and relative humidity on shortwave radiative forcing by aerosols has recently been examined by Pilinis *et al.* (1995) and Nemesure *et al.* (1995).

Scattering efficiency. The quantity $\alpha_{SO_4^{2-}}^{RH_r}$ and the value for this quantity given by Charlson *et al.* (1992), 5 m^2 (g, SO_4^{2-})$^{-1}$, were meant to represent the light scattering efficiency of incremental sulfate aerosol including its associated cations at a low reference relative humidity (typically 30%) or, more formally, the derivative of light scattering coefficient with respect to sulfate mass concentration. The basis for selection of this value is given by Charlson *et al.* (1992) and is further elaborated upon by Anderson *et al.* (1994). However, both appropriateness of the definition of the quantity and its magnitude have been questioned (Hegg *et al.*, 1993, 1994). Since the sulfate ion in aerosol particles is inevitably associated with other aerosol substances, the definition given by Charlson *et al.*, would seem reasonable for the purpose of assessing the climate forcing of aerosol sulfate. One sticking point is how to account for other aerosol processes associated with formation of sulfate aerosol. For example, accretion of sulfate by a pre-existing aerosol, such as ammonium nitrate, may release nitrate into the atmosphere (as HNO_3), thereby decreasing the incremental aerosol mass that can be attributed to the sulfate. For this reason Hegg *et al.* prefer a definition that refers only to the sulfate ion and would treat the climate forcing of all aerosol substances separately and additively. Ultimately treatment of these phenomena must be refined, by utilization of models that explicitly treat chemical interactions of aerosol species (e.g. Kim *et al.*, 1993a, b). In the present discussion we retain the convention of Charlson *et al.*, but call attention to the issue raised by Hegg. With this convention, the value 5 m^2 (g SO_4^{2-})$^{-1}$ uncertain to a factor of 1.5 seems a reasonable default value for climate calculations. However, the large uncertainty range of that estimate (more than a factor of 2 between extremes) is clearly unsatisfactory for purposes of assessing aerosol influences on climate. Finally, it must be stressed that the mass scattering efficiency is not a fundamental property of a material (such as index of refraction) but, as we shall see, depends strenuously on particle size and hence on the size distribution of the aerosol.

The dependence of the mass scattering efficiency on particle diameter is shown in Fig. 5 for a dry ammonium sulfate aerosol. Here the quantity plotted is the light scattering efficiency per sulfate mass, consistent with the notation of equation (1). As may be seen from the figure the mass scattering efficiency of the aerosol exhibits a wide range of values in the

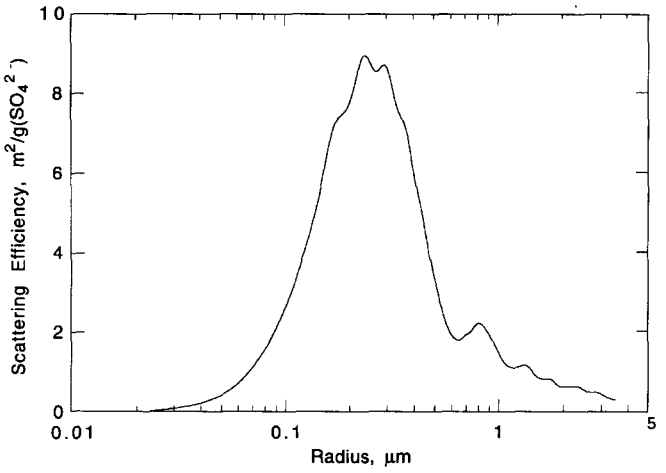

Fig. 5. Dependence of light scattering efficiency of ammonium sulfate on particle radius. Wavelength, 0.53 μm; index of refraction 1.53. Light scattering efficiency is expressed in units m^2 $(g\,SO_4^{2-})^{-1}$. Modified from Ouimette and Flagan (1982).

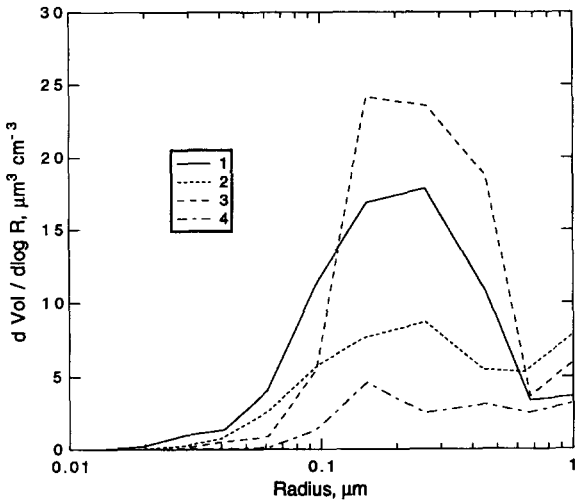

Fig. 6. Equal area plots of volume distribution of aerosols measured from shipboard during a transect across the North Atlantic. Distributions 1–4 exhibit transition from largely continental aerosol (1) to largely marine aerosol (4). Data from Hoppel *et al.* (1990).

size range encompassed by accumulation mode aerosols. Particle size is thus a key determinant of light scattering efficiency. The maximum value, 9 m^2 $(g\ SO_4^{2-})^{-1}$, which occurs at particle diameter roughly equal to the wavelength, is somewhat greater than the value employed in Table 1, 5 m^2 $(g\ SO_4^{2-})^{-1}$; the average value for an actual ambient aerosol would depend on the size distribution of the aerosol.

To pursue this further, Fig. 6 shows several size distributions of submicrometer aerosols measured over the North Atlantic (Hoppel *et al.*, 1990). The measurements were made at a fairly low instrumental relative humidity of 11–27% below ambient. The several distributions 1–4 given in the figure represent decreasing continental character and increasing marine character of the aerosol as the measurements were made at increasing distances from the North American coast, and as established by back-trajectory analysis. The distributions are truncated at 1 μm because larger particles were highly correlated with wind speed, indicative of soil dust and/or sea salt origin. The mean scattering efficiency for the several distributions, evaluated with the mass scattering efficiency of ammonium sulfate given in Fig. 5 gives ranges from 4.9 to 6.0 m^2 $(g\ SO_4^{2-})^{-1}$, consistent with the value 5 m^2 $(g\ SO_4^{2-})^{-1}$ given in Table 1.

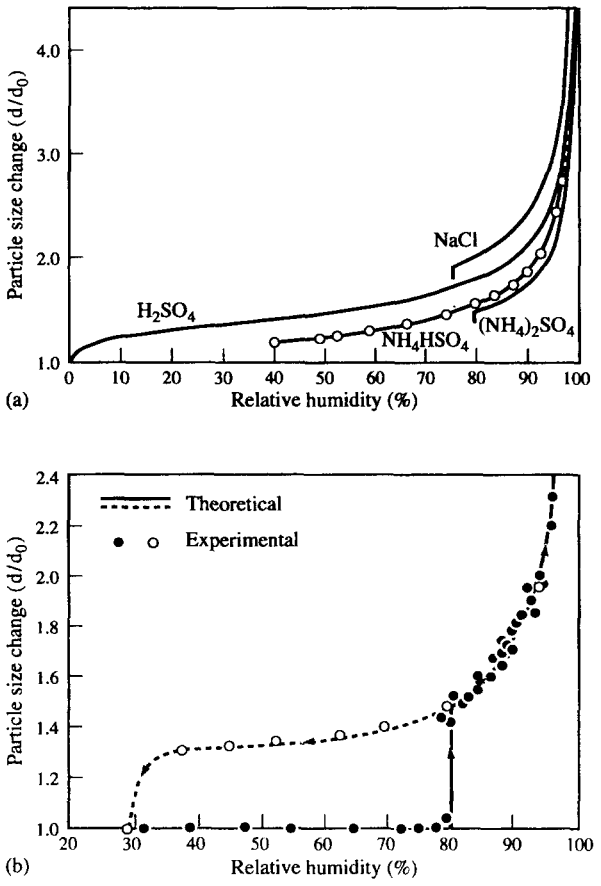

Fig. 7. Dependence of aerosol particle radius on relative humidity: (a) theoretical curves showing deliquescence points for several salts; (b) theory and observations for ammonium sulfate, showing supersaturation regime exhibited on decreasing RH below deliquescence point (Tang and Munkelwitz, 1977; Tang, 1980).

Relative humidity dependence of light scattering efficiency. A second major influence on the magnitude of direct light scattering by aerosols is the dependence of their size, and hence scattering efficiency relative to dry mass, on relative humidity arising from accretion of water by deliquescent aerosol components. The dependence of scattering efficiency on RH is indicated in equation (1) by the factor $f(\mathrm{RH})$. In examining this dependence we focus again on sulfate as an example. Figure 7 shows this dependence for several sulfate species. Figure 7(a), showing the dependence exhibited with increasing RH, displays the abrupt increase in size associated with deliquescence, occurring at a RH corresponding to the vapor pressure of water above a saturated solution. As indicated in Fig. 7(b), as RH decreases, an aerosol particle can remain as a supersaturated solution to relative humidities well below the deliquescence point. Such behavior is commonly observed in tropospheric aerosols (Rood *et al.*, 1989; Koloutsou-Vakakis and Rood, 1994). The RH dependence of particle size may be calculated for known composition using expressions based either directly on measurements (e.g. Tang and Munkelwitz, 1991, 1994) or on multicomponent thermodynamic equilibria (e.g. Kim *et al.*, 1993a, b).

Figure 8 shows the effect of dry particle size and relative humidity in combination, illustrating the dependence of scattering efficiency, i.e. the quantity $f(\mathrm{RH}) \times \alpha(\mathrm{RH_r})$, having units $\mathrm{m^2\ (g\ SO_4^{2-})^{-1}}$, upon particle dry radius and RH. The substantial increase in scattering efficiency with increasing RH should be noted; see also Garland (1969). At 83% RH, for example, the scattering efficiency reaches a maximum of $\sim 20\ \mathrm{m^2\,g^{-1}}$, compared to the value $f(\mathrm{RH}) \times \alpha(\mathrm{RH_r}) = 8.5\ \mathrm{m^2\,g^{-1}}$ employed in the evaluation given in Table 1. For a sulfate concentration of 4 $\mu\mathrm{g\,m^{-3}}$, representative of the remote, anthropogenically

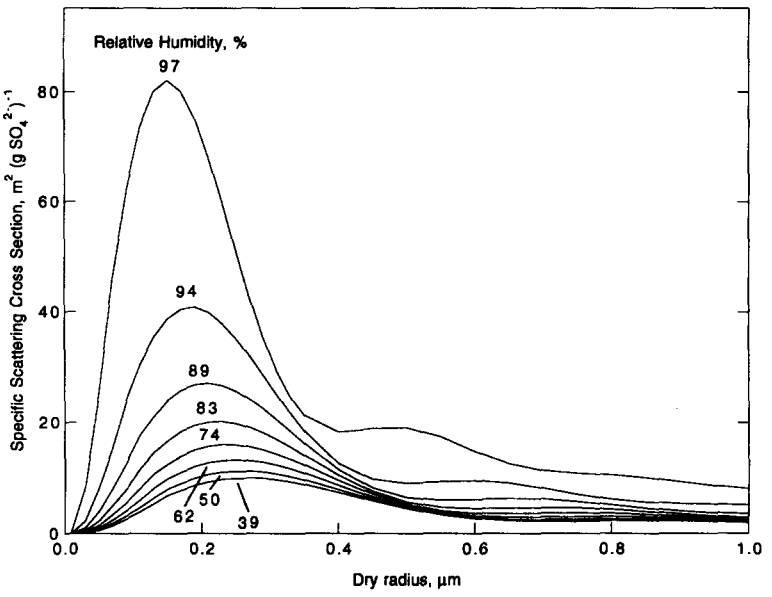

Fig. 8. Dependence of specific extinction coefficient of aqueous ammonium sulfate aerosol on particle dry "radius" (radius of a sphere of equal volume) for indicated values of relative humidity. Calculated from density, vapor pressure, and index of refraction data of Tang and Munkelwitz (1994). In order to suppress high frequency resonances a gamma size distribution with a very narrow effective width was employed for each of the particle sizes; wavelength, 0.65 μm. Unpublished calculations by S. Nemesure.

influenced troposphere (mixing ratio 1 nmol mol_{air}^{-1}, i.e. 1 ppb), uniformly distributed through 2 km (sulfate column burden 4 mg m^{-2}), the corresponding aerosol optical depth is 0.16. It is clear from this magnitude of the relative humidity dependence that accurate representation of the direct forcing will require representing this relative humidity dependence. It may also be noted that any correlation between mass loading and relative humidity will result in a strong bias in light scattering estimated using mean values for sulfate loading and relative humidity.

Upscatter fraction. Aerosol microphysics also influences the radiative forcing through the upscatter fraction β, which exhibits a dependence on particle size as a consequence of the particle size dependence of the phase function, i.e. the angular distribution of scattered radiation. These phase functions are illustrated in Fig. 9 for several particle sizes. At small radius the phase function is symmetric in the forward and back directions, but with increasing particle radius the light is scattered increasingly in the forward direction. Since the incident radiation comes from the upward direction, a shift toward forward scattering decreases the upscatter fraction.

Expressions for evaluation of β on particle radius and solar zenith angle were given by Wiscombe and Grams (1976). The fraction of light that is scattered into the upward hemisphere is given by the fraction of the integral over the phase function that is in the upward hemisphere. Note that it is the upward hemisphere that is important, not the back hemisphere relative to the direction of the incident radiation, and for this reason the term *upscatter fraction* may be preferable to the frequently used "backscatter fraction". The distinction is illustrated in Fig. 10, which shows the scattering geometry. Here θ_0 is the solar zenith angle, the direction of the incident radiation, as measured from the vertical; θ represents the scattering angle about the incident direction.

Scattering is assumed isotropic relative to the azimuthal angle ϕ, but note that the angle of the scattered radiation as measured from the vertical, α, does depend on ϕ, as indicated by the several azimuthal angles shown in the figure, ϕ, ϕ', ϕ'', and ϕ'''. In the figure scattering is in the upward hemisphere for ϕ between ϕ' and ϕ'''. The upscatter fraction for

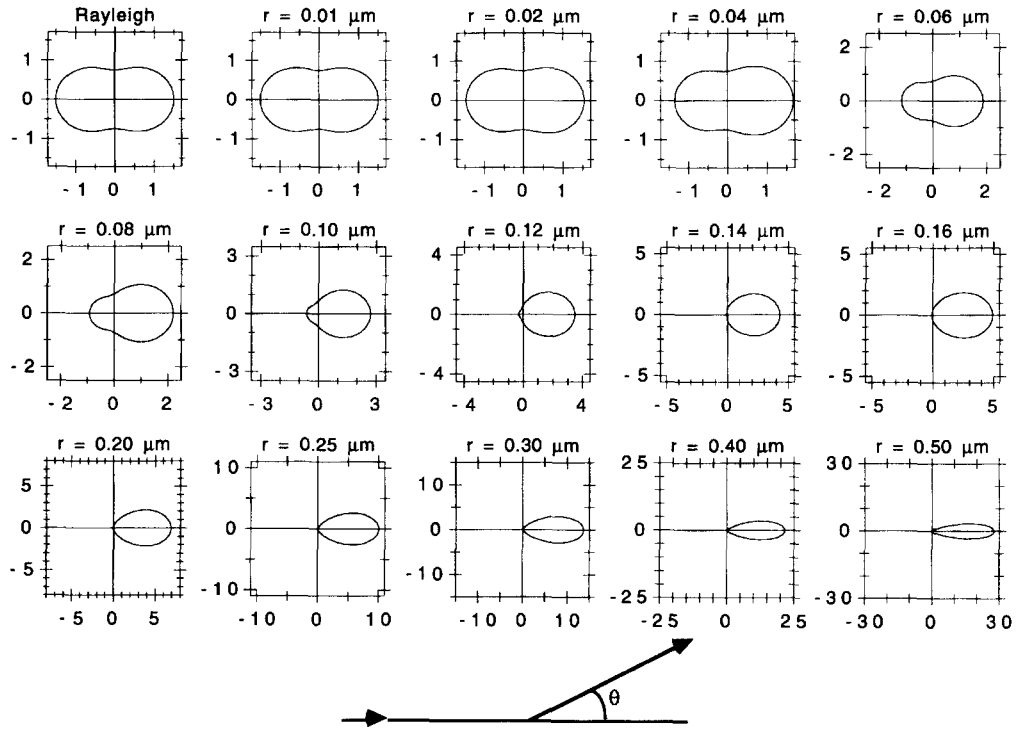

Fig. 9. Polar plots of scattering phase functions $P(\theta)$ as a function of particle radius illustrating the transition, with increasing particle radius, from equal scattering in the forward and back directions to scattering peaked in the forward direction. Wavelength of incident radiation was 0.55 μm, index of refraction 1.52–0.008i. In order to suppress high frequency resonances a gamma size distribution with a very narrow effective width was employed for each size. Note that the plots are on a linear scale rather than the customary log scale (e.g. Twomey, 1977). Unpublished calculations by R. Wagener.

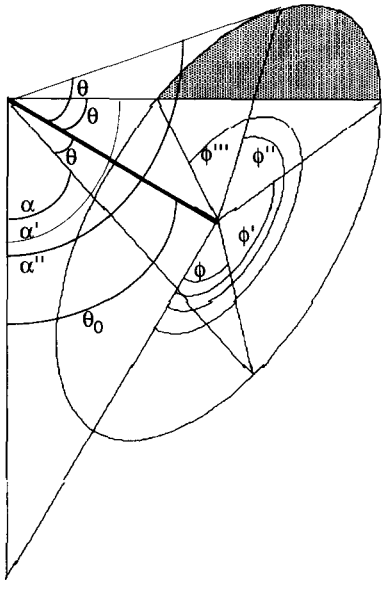

Fig. 10. Scattering geometry defining upscatter fraction. The bold line extending from the upper left of the figure denotes the direction of the incident radiation, with zenith angle θ_0. Radiation is scattered from this incident direction with angle θ and azimuthal angle ϕ. Scattering vectors are drawn for several indicated values of ϕ for a single value of θ. For each of these scattering vectors are α denotes the zenith angle of the scattered radiation. Note that for ϕ between ϕ' and ϕ''' (example ϕ'') scattering is into the upward hemisphere (example α'').

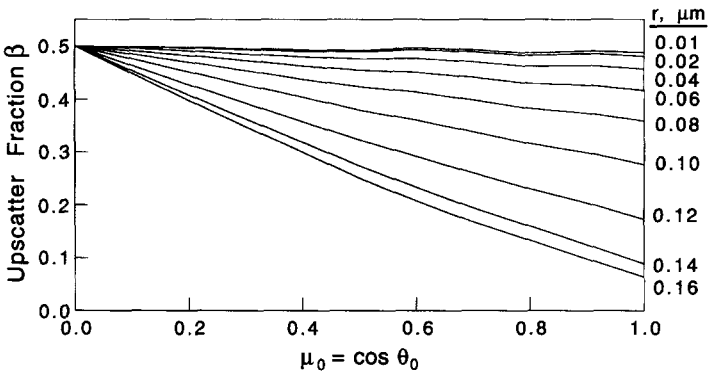

Fig. 11. Fraction of incident radiation scattered into the upward hemisphere β as a function of cosine of solar zenith angle for indicated values of particle radius. Evaluation is for wavelength 0.55 μm. Unpublished calculations by R. Wagener.

a given solar zenith angle θ_0 is given by the integral over scattering angle $d\Omega \equiv \sin\theta\, d\theta\, d\phi$

$$\beta(\theta_0) = \int_{\substack{\text{upward}\\ \text{hemisphere}}} P(\theta, \phi)d\Omega \Big/ \int_{4\pi} P(\theta, \phi)d\Omega = \int_{\cos\alpha < 0} P(\theta, \phi)d\Omega/4\pi. \tag{4}$$

As shown by Wiscombe and Grams (1976), and as may readily be shown from geometrical considerations (by twice application of the law of cosines; cf. Fig. 10),

$$\beta(\theta_0) = (2\pi)^{-1} \int_{\pi/2-\theta_0}^{\pi/2+\theta_0} P(\theta) \sin\theta \cos^{-1}(\cot\theta_0 \cot\theta)\, d\theta + \frac{1}{2}\int_{\pi/2+\theta_0}^{\pi} P(\theta)\sin\theta\, d\theta. \tag{5}$$

The dependence of β on θ_0 and particle radius r is examined in Fig. 11 as a function of the cosine of the solar zenith angle, μ_0. For the sun at the horizon ($\mu_0 = 0$) β is 0.5, independent of r, as required by symmetry; for the sun increasingly higher in the sky, forward scattering by larger particles leads to a decrease in β.

In order to evaluate the average radiative forcing of the aerosol, it is necessary to average β appropriately over solar zenith angle; here we assume the aerosol is uniformly distributed geographically. For such an average one needs to consider the power-weighted average. The incident solar radiant intensity normal to the surface decreases with increasing solar zenith angle as $\cos\theta_0$. However, for an optically thin aerosol the effective scattering path length increases as sec θ_0, so that the two effects just cancel. Consequently, the appropriate average over the illuminated hemisphere can be estimated as

$$\bar{\beta} = \int_0^1 \beta\, d\mu_0 \Big/ \int_0^1 d\mu_0 = \int_0^1 \beta\, d\mu_0 \tag{6}$$

where $d\mu_0 = d\cos\theta_0 = -\sin\theta_0\, d\theta_0$. The result of the integration is shown in Fig. 12 as a function of particle radius. Also shown in the figure is the value $\bar{\beta} = 0.29$ used in the estimate of global average forcing of Charlson *et al.* (1992) and the 30% uncertainty given by those investigators. It may be seen that in the important radius range 0.1–0.4 μm (cf. Fig. 6) $\bar{\beta}$ varies essentially over that entire range. To explore this further, Fig. 13 shows a plot of the product of scattering cross section per unit mass loading α times hemispheric average upscatter fraction $\bar{\beta}$, averaged over the solar spectrum. (It should be noted for comparison with earlier figures that in this figure the quantity a represents the scattering cross-section per unit mass of particle, not per unit mass of sulfate.) Once again the strong dependence on particle radius is noted, as dominated by the influence of the particle size dependence of α, Figs 5 and 8. For particles within the radius range 0.1–0.6 μm the average can be taken as 0.58 $m^2\, g^{-1}$, uncertain to 30%.

Figure 14 shows the result of averaging the forcing over the sunlit fraction of the diurnal cycle to evaluate the 24-hour average forcing at a midlatitude location. Here the forcing, normalized to a unit mass of sulfate aerosol (W m^{-2} per gram sulfate m^{-2}, or W

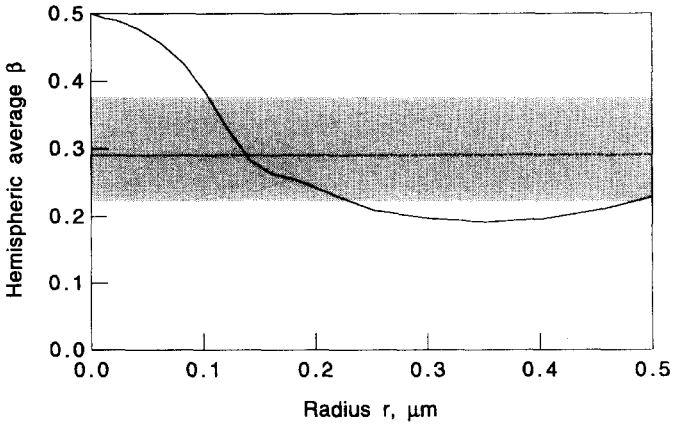

Fig. 12. Hemispheric-average fraction of upscattered radiation $\bar{\beta}$ as a function of particle radius. Evaluation is for wavelength 0.55 μm. Horizontal line and stippled band indicate value of $\bar{\beta} = 0.29$ uncertain to a factor of 1.3 given by Charlson *et al.* (1992).

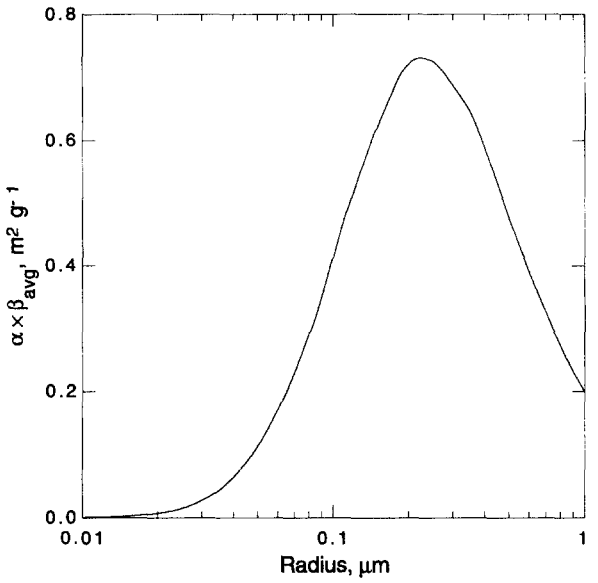

Fig. 13. Product of the total light scattering coefficient per unit aerosol mass α times the hemispheric-average upscatter fraction $\bar{\beta}$, as averaged over the solar spectrum, as a function of particle radius. Single scattering without aerosol absorption is assumed. Evaluated from calculations presented by Wiscombe and Grams (1976).

$(g\,SO_4^{2-})^{-1}$), is shown for $(NH_4)_2SO_4$ aerosol at 83% RH as a function of particle dry raidus. Similar plots can be generated for other values of RH; cf. Fig. 8. A rather broad maximum (negative) forcing is exhibited for $r_{dry} \approx 0.1$ μm. The magnitude of the forcing exhibits a seasonal dependence, governed largely by length of day. For sulfate column burden 8 mg m^{-2} (cf. the example calculation of NH-average loading given above), the corresponding 24-hour average forcing is ~ 3 W m^{-2}, depending on season. It should be noted that this calculation is for clear sky; the average forcing would be less, by a factor of about 0.4, for typical cloud-free sky fraction of 40%.

Finally it should be noted that the several figures (Figs 5, 8, 13 and 14) showing aerosol optical and radiative properties as a function of radius are meant to illustrate the radius dependence of these quantities, and not to imply that the properties of a given aerosol can be represented by the properties corresponding to a single radius value. In order to determine the value of a given optical or radiative property for a particular aerosol, it is necessary to convolve the radius dependence of the property with the size distribution of the

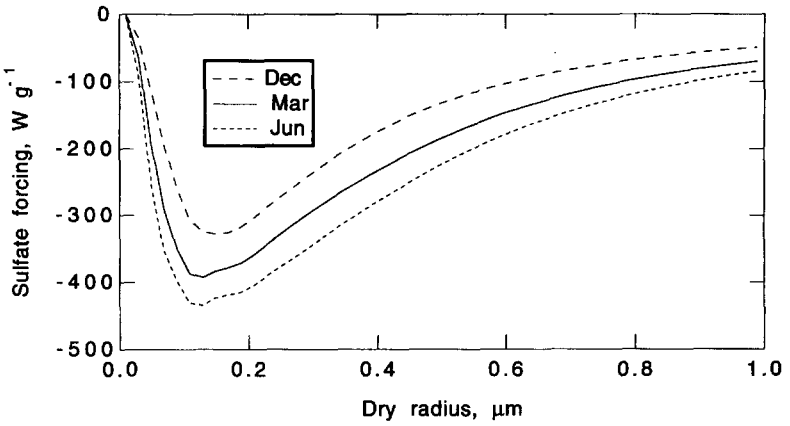

Fig. 14. Dependence of normalized shortwave forcing (W m^{-2} per $g(SO_4^{2-})m^{-2}$) of sulfate aerosol on particle radius. Normalized forcing represents the 24-hour mean for the 15th of the indicated month for a cloud-free sky, for relative humidity 83%. Latitude 36.7°N; surface albedo 0.11. Single scattering without aerosol absorption is assumed. Unpublished calculations by S. Nemesure.

aerosol, as was done above in evaluating the mean scattering cross-section for the several size distributions given in Fig. 6. For an optically thin aerosol this may be achieved to good approximation by treating the radius dependence given in each of the several figures as a Green's function kernel for the integration.

DISCUSSION

The foregoing discussion has focused on the two principal sources of uncertainty in describing the radiative forcing by aerosols by direct light scattering, namely, uncertainty in the aerosol mass loading and uncertainty in the forcing per mass loading. In fact, the latter uncertainty attaches not so much to the radiative forcing calculation *per se*, as to the uncertainty in or variability of the microphysical properties of the aerosol, mainly size distribution. This conclusion applies not just to box-model calculations but equally to calculations of forcing based on modeled geographical distributions of the aerosol, since estimates of forcing obtained with such modeled distributions are subject to the same sensitivity to loading and particle size as are the box-model calculations. It may thus be seen that any substantial reduction in the uncertainty in this forcing will require improved description, by modeling or by measurement from satellite borne instruments, of the loading, composition, and size distribution of anthropogenic aerosols.

The estimates of shortwave radiative forcing of climate by direct light scattering by anthropogenic aerosols given by box-model calculations described here establish that this forcing is substantial, even in global average, in the context of greenhouse gas forcing. The uncertainty associated with the aerosol forcing, both direct and indirect, is the greatest uncertainty associated with anthropogenic influences on climate. Nonetheless, present best estimates indicate that the aerosol forcing cannot be sufficiently small as to be insignificant in the context of the totality of anthropogenic forcing.

Because of the localization of aerosol loadings in and downwind of industrial sources, mainly in North America, Europe, and eastern Asia, much greater forcing may be expected in these regions than in the global mean (e.g. Kiehl and Briegleb, 1993). In order to evaluate this, it is necessary to account for the geographical distribution of the aerosol loading by means of models that describe the transport, transformation, and removal processes that control the loadings of these aerosols in the atmosphere. In principle such models can also account for correlations among the several variables governing the aerosol forcing, for example, mass loading, particle size, cloud cover, and relative humidity. However, confident application of such models requires evaluation of their accuracy by comparison of modeled and measured aerosol loadings and other properties such as size distribution and state of

neutralization. Because of the high degree of spatial and temporal variability of this loading, it appears that sensitive evaluations of chemical models will be obtainable only when comparing observations to quantities calculated with models driven by meteorological wind and precipitation fields that are derived from observations. Investigations with such models are now being undertaken for this purpose (Benkovitz *et al.*, 1994). Results from these models can be compared to *in situ* measurements and to measures of aerosol optical depth derived from satellite instruments. Once suitable evaluated chemical models are at hand, they can be used with somewhat greater confidence in examining the climatic influence of these aerosols. In view of different aerosol properties depending on their sources, e.g., differences in size distributions for continental versus marine aerosols (Hoppel *et al.*, 1990) and differences in relative humidity growth curves as a function of relative humidity (Tang and Munkelwitz, 1991, 1994), future chemical modeling efforts should aim toward explicitly representing these properties in addition to mass loading.

Despite the importance of these aerosol influences on climate change inferred from estimates of the magnitude of the forcing, there is as yet relatively little observational information that reliably and confidently can be used to support these estimates. Locally and in a few instances the direct radiative influence of atmospheric aerosols has been demonstrated and its magnitude related to the aerosol loading (Russell *et al.*, 1979; Ball and Robinson, 1982). There is also indication from satellite measurements of enhanced aerosol loading over the western North Atlantic and western North Pacific that is attributed to aerosols exported from industrial regions (Rao *et al.*, 1989). There is also rather convincing evidence of the radiative influence of stratospheric aerosols arising from the eruption of the volcano Pinatubo in the Philippines in June 1991 (Dutton and Christy, 1992; Minnis *et al.*, 1993; McCormick *et al.*, 1995); these observations confirm, in a broad way, the phenomenon of shortwave radiative forcing by aerosols. However, much more work is required to narrow substantially the uncertainty in forcing due to anthropogenic aerosols. Unfortunately, the existing class of satellite radiometers is only marginally sensitive to contributions to radiance due to these aerosols (Hansen *et al.*, 1993; Penner *et al.*, 1994; Wagener *et al.*, 1996). Ultimately a variety of closure experiments that test models of components of the process is required to build confidence in model evaluations of the aerosol forcing (Penner *et al.*, 1994).

A potentially attractive approach to looking for evidence of aerosol forcing of climate is through examination for possible climate changes that may be attributable to this forcing. Such influences might be manifested through interhemispheric differences or regional patterns in temperature anomaly trend, or in seasonal or diurnal patterns in these trends. Indeed several such patterns have been identified as plausibly attributable to aerosol forcing (Engardt and Rodhe, 1993; Hunter *et al.*, 1993). Karl and colleagues have noted that aerosol forcing, being operative during daylight hours might also lead to a differential temperature anomaly trend in daily maximum and minimum temperatures (usually daytime and nighttime, respectively) that might account for the lesser rate of warming in daytime observed in several industrial regions (Karl *et al.*, 1993, 1995). Although such arguments are plausible, it does not appear possible at the present stage of understanding of climate response to forcing, taking into account processes such as heat transport through atmospheric and oceanic circulation patterns, to unequivocally ascribe such patterns to aerosol forcing. A possible exception may be the response to large, short-term perturbations, i.e. volcanoes, such as Pinatubo, for which the time signature of the forcing and response may permit such unequivocal attribution. Recent climate modeling studies indicate that the apparent global cooling following the Pinatubo eruption (Dutton and Christy, 1992) is consistent with a response to this aerosol forcing and thereby lend credibility to the theoretical arguments indicating substantial climate forcing by anthropogenic tropospheric aerosols (Hansen *et al.*, 1992; Lacis and Mishchenko, 1995).

The uncertainty in the magnitude of radiative forcing due to anthropogenic aerosols is of major import with respect to developing empirical relations between radiative forcing and climate system response. Studies of temperature trends over the industrial period (summarized by Folland *et al.*, 1992) indicate an increase in global mean temperature over this

period of about 0.5 K. If only the greenhouse forcing is considered, it is superficially tempting to relate this increase to the greenhouse forcing and to adduce this relation as empirical evidence for climate change due to the enhanced greenhouse effect. It is now becoming recognized that the whitehouse forcing is comparable to the greenhouse forcing and that empirical relations of temperature trend and forcing must take the whitehouse forcing into account (e.g. Wigley and Raper, 1992). However, as is apparent from Fig. 2, the uncertainty associated with the whitehouse forcing is so great as to entirely undermine the ability to draw such relations. Clearly, unless and until the uncertainty in the whitehouse forcing is substantially reduced, any arguments relating global temperature trend to forcing over the industrial period, either qualitative or quantitative, must be placed on hold.

One final point that should be noted regarding the aerosol forcing in the context of the broader climate change issue has to do with the vastly different atmospheric residence times of the aerosol particles responsible for the whitehouse effect (about a week) compared to the infrared gases responsible for the greenhouse effect (decades to centuries). This difference in lifetimes means that to whatever extent shortwave radiative forcing by anthropogenic aerosols is offsetting longwave forcing by anthropogenic greenhouse gases, it is aerosols from a week's worth of emissions that are offsetting forcing by greenhouse gases resulting from decades' worth of emissions. Recognition of this leads to the immediate realization in the inherent unworkability of any scheme to take deliberate advantage of the aerosol forcing as a mechanism for offsetting the forcing due to increased concentrations of greenhouse gases.

Acknowledgements—This paper is based on a presentation at the specialty conference "Aerosols and Atmospheric Optics: Radiation Balance and Visual Air Quality", Snowbird, UT, 26–30, September 1994, sponsored by the Air and Waste Management Association and the American Geophysical Union. I thank S. Nemesure and R. Wagener for calculations and C. Benkovitz for preparation of Table 2. This research was supported by the Environmental Sciences Division of the U.S. Department of Energy (DOE) as part of the Atmospheric Radiation Measurement Program and was performed under the auspices of DOE under Contract No. DE-AC02-76CH00016.

REFERENCES

Anderson, T. L., Charlson, R. J., White, W. H. and McMurry, P. H. (1994) Comment on "Light scattering and cloud condensation nucleus activity of sulfate aerosol measured over the Northeast Atlantic Ocean" by D. A. Hegg *et al. J. geophys Res.* **99,** 25,947–25,949.

Andreae, M. O. (1995) Climate effects of changing atmospheric aerosol levels. In *World Survey of Climatology*, Vol. XVI, *Future Climate of the World* (Edited by Henderson-Sellers, A.). Elsevier, New York (in press).

Balkanski, Y. J., Jacob, D. J., Gardner, G. M., Graustein, W. C. and Turekian, K. K. (1993) Transport and residence times of tropospheric aerosols inferred from a global three-dimensional simulation of ^{210}Pb. *J. geophys. Res.* **98,** 20,573–20,586.

Ball, R. J. and Robinson, G. D. (1982) The origin of haze in the central United States and its effect on solar irradiation. *J. appl. Meterol.* **21,** 171–188.

Benkovitz, C. M., Berkowitz, C. M., Easter, R. C., Nemesure, S., Wagener, R. and Schwartz, S. E. (1994a) Sulfate over the North Atlantic and adjacent continental regions: evaluation for October and November 1986 using a three-dimensional model driven by observation-derived meteorology. *J. geophys. Res.* **99,** 20,725–20,756.

Bondietti, E. A., Brantley, J. N. and Rangarajan, C. (1988) Size distributions and growth of natural and Chernobyl-derived submicron aerosols in Tennessee. *J. envir. Radioactivity* **6,** 99–120.

Boucher, O. and Anderson, T. L. (1995) GCM assessment of the sensitivity of direct climate forcing by anthropogenic sulfate aerosols to aerosol size and chemistry. *J. geophys. Res.* **100,** 26,117–26,134.

Burkhard, E. G., Dutkiewicz, V. A. and Husain, L. (1994) A study of SO_2, SO_4^{2-} and trace elements in clear air and clouds above the midwestern United States. *Atmos. Envir.* **28,** 1521–1533.

Cambray, R. S., Cawse, P. A., Garland, J. A., Gibson, J. A. B., Johnson, P., Lewis, G. N. J., Newton, D., Salmon, L. and Wade, B. O. (1987) Observations on radioactivity from the Chernobyl accident. *Nucl. Energy* **26,** 77.

Carmichael, G., Peters, L. K. and Saylor, R. D. (1991) The STEM-II regional scale acid deposition and photochemical oxidant model—I. An overview of model development and applications. *Atmos. Envir.* **25A,** 2077–2090.

Chang, J. S., Brost, R. A., Isaksen, I. S. A., Madronich, S., Middleton, P., Stockwell, W. R. and Walcek, C. J. (1987) A three-dimensional Eulerian acid deposition model: physical concepts and formulation. *J. geophys. Res.* **92,** 14,681–14,700.

Charlson, R. J. and Heintzenberg, J. Eds. (1995) *Aerosol Forcing of Climate.* Wiley, New York.

Charlson, R. J., Langner, J., Rodhe, H., Leovy, C. B. and Warren, S. G. (1991) Perturbation of the Northern Hemisphere radiative balance by backscattering from anthropogenic aerosols. *Tellus* **43AB,** 152–163.

Charlson, R. J., Schwartz, S. E., Hales, J. M., Cess, R. D., Coakley, J. A. Jr., Hansen, J. E. and Hofmann, D. J. (1992) Climate forcing by anthropogenic aerosols. *Science* **255,** 423–430.

Coakley, J. A. Jr., Cess, R. D. and Yurevich, F. B. (1983) The effect of tropospheric aerosols on the earth's radiation budget: a parameterization for climate models. *J. atmos. Sci.* **40,** 116–138.

Cox, S. J., Wang, W.-C. and Schwartz, S. E. (1995) Climate response to radiative forcings by aerosols and greenhouse gases. *Geophys. Res. Lett.* **22,** 2509–2512.

Daum, P. H. (1988) Processes determining cloudwater composition: inferences from field measurements. In *Acid Deposition at High Elevation Sites* (Edited by Unsworth, M. H. and Fowler, D.), pp. 139–153. Kluwer, Dordrecht.

Daum, P. H., Kelly, T. J., Schwartz, S. E. and Newman, L. (1984) Measurements of the chemical composition of stratiform clouds. *Atmos. Envir.* **18,** 2671–2684.

Dutton, E. G. and Christy, J. R. (1992) Solar radiative forcing at selected locations and evidence for global lower tropospheric cooling following the eruptions of El Chichón and Pinatubo. *Geophys. Res. Lett.* **19,** 2313–2316.

Engardt, M. and Rodhe, H. (1993) A comparison between patterns of temperature trends and sulfate aerosol pollution. *Geophys. Res. Lett.* **20,** 117–120.

Erickson, D. J. III., Walton, J. J., Ghan, S. J. and Penner, J. E. (1991) Three-dimensional modeling of the global atmospheric sulfur cycle: a first step. *Atmos. Envir.* **25A,** 2513–2520.

Folland, C. K., Karl, T. R., Nicholls, N., Nyenzi, B. S., Parker, D. E. and Vinnikov, K. Ya. (1992) Observed climate variability and change. In *Climate Change 1992: The Supplementary Report to the IPCC Scientific Assessment* (Edited by Houghton, J. T., Callander, B. A. and Varney, S. K.). Cambridge Univ. Press, Cambridge, U.K.

Forgan, B. W. (1987) Aerosol optical depth. In *Baseline Atmospheric Program (Australia) 1985* (Edited by Forgan, B. W. and Fraser, P. J.), p. 56. Department of Science/Bureau of Meteorology and CSIRO/Division of Atmospheric Research, Australia.

Garland, J. A. (1969) Condensation on ammonium sulphate particles and its effect on visibility. *Atmos. Envir.* **3,** 347–354.

Giorgi, F. and Chameides, W. L. (1986) Rainout lifetimes of highly soluble aerosols and gases as inferred from simulations with a general circulation model. *J. geophys. Res.* **91,** 14,367–14,376.

Hansen, J., Lacis, A., Ruedy, R. and Sato, M. (1992) Potential climate impact of Mount Pinatubo eruption. *Geophys Res. Lett* **19,** 215–218.

Hansen, J., Rossow, W. and Fung, I. (1990) The missing data on global climate change. *Issues Sci. Technol.* **7,** 62–69.

Hansen, J., Rossow, W. and Fung, I. (1993) Long-term monitoring of global climate forcings and feedbacks. *Proc. Workshop GISS, Feb. 3–4, 1992.* NASA Conference Publication 3234.

Hass, H., Jakobs, H. J., Memmesheimer, M., Ebel, A. and Chang, J. S. (1991) Simulation of a wet deposition case in Europe using the European acid deposition model (EURAD). In *Air Pollution Modeling and Its Application VIII* (Edited by van Dop, H. and Steyn, D. G.), pp. 205–213. Plenum, New York.

Hegg, D. A., Ferek, R. J. and Hobbs, P. V. (1993) Light scattering and cloud condensation nucleus activity of sulfate aerosol measured over the Northeast Atlantic Ocean. *J. geophys. Res.* **98,** 14,887–14,894.

Hegg, D. A., Ferek, R. J. and Hobbs, P. V. (1994) Reply [to comment by T. L. Anderson *et al.*]. *J. geophys. Res.* **99,** 25,951–25,954.

Hoppel, W. A., Fitzgerald, J. W., Frick G. M., Larson, R. E. and Mack, E. J. (1990) Aerosol size distributions and optical properties found in the marine boundary layer over the Atlantic Ocean. *J. geophys. Res.* **95,** 3659–3686.

Hunter, D. E., Schwartz, S. E., Wagener, R. and Benkovitz, C. M. (1993) Seasonal, latitudinal, and secular variations in temperature trend: evidence for influence of anthropogenic sulfate. *Geophys. Res. Lett.* **20,** 2455–2458.

Husain, L. and Dutkiewicz, V. A. (1990) A long-term (1975–1988) study of atmospheric SO_4^{2-}: regional contributions and concentration trends. *Atmos. Envir.* **24A,** 1175–1187.

IPCC (Intergovernmental Panel on Climate Change) (1990) In *The IPCC Scientific Assessment* (Edited by Houghton, J. T., Jenkins, G. J. and Ephraums, J. J.), pp. 41–68. Cambridge University Press, Cambridge.

IPCC (Intergovernmental Panel on Climate Change) (1992) Houghton, J. T., Callander, B. A. and Varney, S. K. Climate Change 1992: *The Supplementary Report to the IPCC Scientific Assessment.* Cambridge Univ. Press, Cambridge.

IPCC (Intergovernmental Panel on Climate Change) (1995) Radiative Forcing of Climate Change. In *Climate Change 1994* (Edited by Houghton, J. T., Meira Filho, L. G., Bruce, J., Lee, H., Callander, B. A., Haites, E., Harris, N. and Maskell, K.), pp. 1–231. Cambridge University Press, Cambridge.

Iverson, T., Saltbones, J., Sandnes, H., Eliassen, A. and Hov, Ø. (1989) Airborne transboundary transport of sulphur and nitrogen over Europe—model descriptions and calculations. Report EMEP MSC-W 2/90, Meteorological Synthesizing Centre–West, Norwegian Meteorological Institute, Oslo.

Jonas, P. R., Charlson, R. J. and Rodhe, H. (1995) Aerosols. In *Climate Change 1994* (Edited by Houghton, J. T., Meira Filho, L. G., Bruce, J., Lee, H., Callander, B. A., Haites, E., Harris, N. and Maskell K.), pp. 127–162. Cambridge University Press, Cambridge.

Karl, T. R., Jones, P. D., Knight, R. W., Kukla, G., Plummer, N., Razuvayev, V., Gallo, K. P., Lindseay, J., Charlson, R. J. and Peterson, T. C. (1993) A new perspective on recent global warming: asymmetric trends of daily maximum and minimum temperature. *Bull. Am. Meteorol. Soc.* **74,** 1007–1023.

Karl, T. R., Knight, R. W., Kukla, G. and Gavin, J. (1995) Evidence for radiative effects of anthropogenic sulfate aerosols in the observed climate record. In *Aerosol Forcing of Climate*, pp. 363–382. Wiley, New York.

Kiehl, J. T. and Briegleb, B. P. (1993) The relative roles of sulfate aerosols and greenhouse gases in climate forcing. *Science* **260,** 311–314.

Kim, Y. P., Seinfeld, J. H. and Saxena, P. (1993a) Atmospheric gas–aerosol equilibrium I. Thermodynamic model. *Aerosol Sci. Technol.* **19,** 157–181.

Kim, Y. P., Seinfeld, J. H. and Saxena, P. (1993b) Atmospheric gas-aerosol equilibrium II. Analysis of common approximations and activity coefficient calculation methods. *Aerosol Sci. Technol.* **19,** 182–198.

Koloutsou-Vakakis, S. and Rood, M. J. (1994) The $(NH_4)_2SO_4$–Na_2SO_4–H_2O system: comparison of deliquescence humidities measured in the field and estimated from laboratory measurements and thermodynamic modeling. *Tellus* **46B,** 1–15.

Lacis, A. A. and Mishchenko, M. I. (1995) Climate forcing: a radiative modeling perspective. In *Aerosol Forcing of Climate* (Edited by Charlson, R. J. and Heintzenberg, J.), pp. 11–42. Wiley, New York.

Langner, J., Bates, T. S., Charlson, R. J., Clark, A. D., Durkee, P. A., Gras, J., Heintzenberg, J., Hofmann, D. J., Huebert, B., Leck, C., Lelieveld, J., Ogren, J. A., Prospero, J., Quinn, P. K., Rodhe, H. and Ryaboshapko, A. G. (1993) The global atmospheric sulfur cycle: an evaluation of model predictions and observations. Report CM-81, Department of Meteorology, Stockholm University, International Meteorological Institute, Stockholm.

Langner, J. and Rodhe, H. (1991) A global three-dimensional model of the tropospheric sulfur cycle. *J. atmos. Chem.* **13,** 225–263.
Luecken, D. J., Berkowitz, C. M. and Easter, R. C. (1992) Use of a three-dimensional cloud-chemistry model to study the transatlantic transport of soluble sulfur species. *J. geophys. Res.* **96,** 22,477–22,490.
McCormick, M. P., Hamill, P., Pepin, T. J ., Chu, W. P., Swissler, T. J. and McMaster, L. R. (1979) Satellite studies of the stratospheric aerosol. *Bull. Am. Meteorol. Soc.* **60,** 1038–1046.
McCormick, M. P., Thomason, L. W. and Trepte, C. R. (1995) Atmospheric effects of the Mt Pinatubo eruption. *Nature* **373,** 399–404.
Milford, J. B. and Davidson, C. I. (1987) The sizes of particulate sulfate and nitrate in the atmosphere—A review. *J. Air Pollut. Contr. Assoc.* **37,** 125–134.
Minnis, P., Harrison, E. F., Stowe, L. L., Gibson, G. G., Denn, F. M., Doelling, D. R. and Smith, W. L. Jr. (1993) Radiative climate forcing by the Mount Pinatubo eruption. *Science* **259,** 411–1415.
Mitchell, J. F. B., Johns, T. C., Gregory, J. M. and Tett, S. F. B. (1995) Climate response to increasing levels of greenhouse gases and sulphate aerosols. *Nature* **376,** 501–504.
Mohnen, V. A. and Kadlecek, J. A. (1989) Cloud chemistry research at Whiteface Mountain. *Tellus* **41B,** 79.
Nemesure, S.,Wagener, R. and Schwartz, S. E. (1995) Direct shortwave forcing of climate by anthropogenic sulfate aerosol: sensitivity to particle size, composition, and relative humidity. *J. geophys. Res.* **100,** 26,105–26,116.
Ouimette, J. R. and Flagan, R. C. (1982) The extinction coefficient of multicomponent aerosols. *Atmos. Envir.* **16,** 2405–2419.
Pandis, S. N., Wexler, A. S. and Seinfeld, J. H. (1995) Dynamics of tropospheric aerosols. *J. Phys. Chem.* **99,** 9646–9659.
Penner, J. E., Charlson, R. J., Hales, J. M., Laulainen, N., Leifer, R., Novakov, T., Ogren, J., Radke, L. F., Schwartz, S. E. and Travis, L. (1994) Quantifying and minimizing uncertainty of climate forcing by anthropogenic aerosols. *Bull. Am. Meteorol. Soc.* **75,** 375–400.
Penner, J. E., Dickinson, R. E. and O'Neill, C. A. (1992) Effects of aerosol from biomass burning on the global radiation budget. *Science* **256,** 1432–1433.
Pilinis, C., Pandis, S. N. and Seinfeld, J. H. (1995) Sensitivity of direct climate forcing by atmospheric aerosols to aerosol size and composition. *J. geophys. Res.* **100,** 18739–18754.
Platnick, S. E. and Twomey, S. (1994) Determining the susceptibility of cloud albedo to changes in droplet concentration with the advanced very high resolution radiometer. *J. appl. Meteorol.* **33,** 334–347.
Ramanathan, V. (1987) The role of earth radiation budget studies in climate and general circulation research. *J. geophys. Res.* **92,** 4075–4095.
Ramanathan, V., Cess, R. D., Harrison, E. F., Minnis, P., Barkstrom, B. R., Ahmad, E. and Hartmann, D. (1989) Cloud-radiative forcing and climate: results from the earth radiation budget experiment. *Science* **243,** 57–63.
Rao, C. R. N., Stowe, L. L. and McClain, E. P. (1989) Remote sensing of aerosols over the oceans using AVHRR data: theory, practice, and applications. *Int. J. Remote Sensing* **10,** 749.
Rao, C. R. N., Stowe, L. L., McClain, E. P. and Sapper, J. (1988) Development and application of aerosol remote sensing with AVHRR data from the NOAA satellites. In *Aerosols and Climate* (Edited by Hobbs, P. V. and McCormick, M. P.), pp. 69–79. Deepak Publishing, Hampton, VA.
Rodhe, H. and Isaksen, I. (1980) Global distribution of sulfur compounds in the troposphere estimated in a height/latitude transport model. *J. geophys. Res.* **85,** 7401–7409.
Rood, M. J., Shaw, M. A., Larson, T. V. and Covert, D. S. (1989) Ubiquitous nature of ambient metastable aerosol. *Nature* **337,** 537–539.
Russell, P. B., Livingston, J. M. and Uthe, E. E. (1979) Aerosol-induced albedo change: measurement and modeling of an incident. *J. atmos. Sci.* **36,** 1587–1608.
Sandnes, H. (1993) Calculated budgets for airborne acidifying components in Europe, 1985, 1987, 1989, 1990, 1991, 1992. Report EMEP MSC-W 1/93, Meteorological Synthesizing Centre-West, Norwegian Meteorological Institute, Oslo.
Schwartz, S. E. (1988) Are global cloud albedo and climate controlled by marine phytoplankton? *Nature* **336,** 441–445.
Schwartz, S. E. (1989) Acid deposition: unraveling a regional phenomenon. *Science* **243,** 753–763.
Schwartz, S. E. and Slingo, A. (1995) Enhanced shortwave cloud radiative forcing due to anthropogenic aerosols. In *Clouds, Chemistry and Climate—Proceedings of NATO Advanced Research Workshop* (Edited by Crutzen, P. and Ramanathan, V.), Springer, Heidelberg (in press).
Slinn, W. G. N. (1983) Air-to sea transfer of particles. In *Air-Sea Exchange of Gases and Particles* (Edited by Liss, P. S. and Slinn, W. G. N.), pp. 299–405. D. Reidel, Dordrecht.
Sloane, C. S. (1983) Optical properties of aerosols–comparison of measurements with model calculations. *Atmos. Envir.* **17,** 409–416.
Spiro, P. A., Jacob, D. J. and Logan, J. A. (1992) Global inventory of sulfur emissions with $1° \times 1°$ resolution. *J. geophys. Res.* **97,** 6023–6036.
Summers, P. W. and Young, J. W. S. (1987) The 'airshed' or 'atmospheric region of influence' for the Great Lakes basin. Presented at the *Int. Joint Commission Symp. "Towards Integrated Monitoring—A Great Lakes Perspective"*, 18th November 1987, Toledo, OH.
Tang, I. N. (1980) Deliquescence properties and particle size change of hygroscopic aerosols. In *Generation of Aerosols* (Edited by Willeke, K.), pp. 153–167. Ann Arbor Science Publishers, Ann Arbor, MI.
Tang, I. N. and Munkelwitz, H. R. (1977) Aerosol growth studies III: ammonium bisulfate aerosols in a moist atmosphere. *J. Aerosol Sci.* **8,** 321–330.
Tang, I. N. and Munkelwitz, H. R. (1991) Simultaneous determination of refractive index and density of an evaporating aqueous solution droplet. *Aerosol Sci. Technol.* **15,** 201–207.
Tang, I. N. and Munkelwitz, H. R. (1994) Water activities, densities and refractive indices of aqueous sulfate and nitrate droplets of atmospheric importance. *J. geophys. Res.* **99,** 18,801–18,808.
Tarrason, L. and Iversen, T. (1992) The influence of North American anthropogenic sulphur emissions over western Europe. *Tellus* **44B,** 114–132.

Taylor, K. E. and Penner, J. E. (1994) Response of the climate system to atmospheric aerosols and greenhouse gases. *Nature* **369,** 734–737.

ten Brink, H. M., Schwartz, S. E. and Daum, P. H. (1987) Efficient scavenging of aerosol sulfate by liquid-water clouds. *Atmos. Envir.* **21,** 2035–2052.

Toon, O. B. and Pollack, J. B. (1976) A global average model of atmospheric aerosols for radiative transfer calculations. *J. appl. Meteorol.* **15,** 225–246.

Twomey, S. (1977) *Atmospheric Aerosols.* Elsevier, New York.

Veefkind, J. P., van der Hage, J. C. H. and ten Brink, H. M. (1995) Nephelometer-derived and measured optical depth: first European closure experiment. *Atmos. Res.* In press.

Venkatram, A. and Karamchandani, P. (1986) Source receptor relationships: a look at acid deposition modeling. *Environ. Sci. Technol.* **20,** 1084–1091.

Wagener, R., Nemesure, S. and Schwartz, S. E. (1996) Aerosol optical depth over oceans: high space and time resolution retrieval and error budget from satellite radiometry. *J. atmos. oceanic Technol.* (submitted).

Whelpdale, D. M., Eliassen, A., Galloway, J. N., Dovland, H. and Miller, J. M. (1988) The transatlantic transport of sulfur. *Tellus* **40B,** 1–15.

White, W. H. (1991) Contributions to Light Extinction. In *Acidic Deposition: State of Science and Technology Report,* Vol. III, Report 24, Section 4, pp. 85–102. National Acid Precipitation Assessment Program (U.S.). Government Printing Office, Washington, DC.

Wigley, T. M. L. and Raper, S. C. B. (1992) Implications for climate and sea level of revised IPCC emissions scenarios. *Nature* **357,** 293–300.

Wiscombe, W. J. and Grams, G. W. (1976) The backscattered fraction in two-stream approximations. *J. atmos. Sci.* **33,** 2440–2451.